Ac Conductivity Measurement of $Cd_5Se_{95-x}Zn_x$ Chalcogenide Semiconductor Using Correlated Barrier Hopping Model

Mohsin Ganaie and M. Zulfequar*
Department of Physics, Jamia Millia Islamia, New Delhi 110025, India

(Received August 9, 2014; in final form May 14, 2015)

$Cd_5Se_{95-x}Zn_x$ ($x = 0, 2, 4, 6$) chalcogenide semiconductors were prepared by conventional melt-quenching and were characterized by X-ray diffraction, scanning electron microscopy, and Fourier transform infrared studies. Ac conductivity of $Cd_5Se_{95-x}Zn_x$ chalcogenide semiconductor has been investigated in the frequency range of 1 kHz–1 MHz and in the temperature range of 290–370 K. The analysis of the experimental results indicates that the ac conductivity is temperature, frequency and concentration dependent. Ac conductivity is found to obey the power law ω^s where $s < 1$. A strong dependence of ac conductivity and exponent s can be well interpreted in terms of correlated barrier hopping model. The maximum barrier height W_m were calculated from the results of dielectric loss according to the Guintini equation that agree with the theory of hopping of charge carriers over potential barrier as suggested by Elliot in case of chalcogenide semiconductors.

DOI: 10.12693/APhysPolA.128.59
PACS: 72.80.Ng, 77.22.–d

1. Introduction

Chalcogenide semiconductor materials have attracted much attention because of their potential application in solid state devices, as new advanced and replaceable technology materials. A variety of applications, present and potential including ultra high density phase change memory, photovoltaic, photoreceivers, photodetector, switching memory, change of electrical resistance and the optical reflectivity [1–7]. Great success has been attained in phase change memories (DVDs), X-ray medical image sensors, highly sensitive vidicons, and xerography. The disordered atomic structure is more flexible and has lower density, and accordingly an include ion may move smoothly, which is promising for application to solid-state batteries. Among various chalcogenide elements only Se is available as amorphous form and glassy ingots at room temperature, but it has disadvantages of short life time and low sensitivity [8]. However the addition of impurities leads to relatively stable glasses with improved physical properties [9–11].

Various authors have studied dc conduction, contact capacitance, spectral properties, ac conduction, structural and magnetic properties of chalcogenide semiconductors [12–16] however the studies on ac conductivities are very limited and require more understanding. Dielectric materials have been the subject of renewed attention. These materials application have been widely employed in various industrial devices such as dynamic access memory, microwave filters, and voltage controlled oscillator and telecommunication technologies. The study of dielectric behavior of chalcogenide semiconductors is expected to reveal structural information, which in effect can be useful for the understanding of the dielectric losses as well. Also the frequency dependent electrical conductivity of chalcogenide semiconductors is important to understand conduction mechanisms in these alloys. So it becomes interesting to study the electrical properties of these materials in ac fields that gives the information about transport in localized states in the forbidden gap [17].

2. Experimental

$Cd_5Se_{95-x}Zn_x$ chalcogenide semiconductors have been prepared by melt-quenching technique. High purities (99.999%) materials have been weighted according to their atomic percentage and sealed in quartz ampoules (length 15 cm and internal diameter 8 mm) under a vacuum 10^6 Torr. The evacuated ampoules then were placed in furnace whose temperature is raised gradually and kept constant 900 °C at a rate of 3–4 °C/min, for 12 h followed by sudden cooling in ice cooled water. The duration of alloying and continuous shaking of the ampoules in the furnace insures the homogeneity in composition. All ampoules were frequently rocked while heating to obtain homogeneous alloys. The quenched samples were removed by breaking the quartz ampoules. The polycrystalline nature of the samples has been ascertained by X-ray diffraction (XRD). The obtained melt were ground into powder form, which is then compressed into pallet (diameter ≈10 mm and thickness ≈1 mm) under a pressure of 5 tons. To avoid poor electrical contact silver paste was used on both sides of the pellets. Ac conductivity, conductance and capacitance were measured by using LCZ (Wayne Kerr 4300 meter). The instrument was used in parallel capacitance mode. The temperature of the pellets was controlled by mounting a heater inside the sample holder and temperature measured by a calibrated chromel–alumel thermocouple near the electrodes. All the measurements were done in a specially designed metallic sample holder under a vacuum of 10^{-3} Torr.

*corresponding author; e-mail: mzulfe@rediffmail.com

3. Results and discussion

3.1. XRD studies

X-ray pattern of the $Cd_5Se_{95-x}Zn_x$ (x = 0, 2, 4, 6) alloy is shown in Fig. 1. X-ray diffraction patterns give

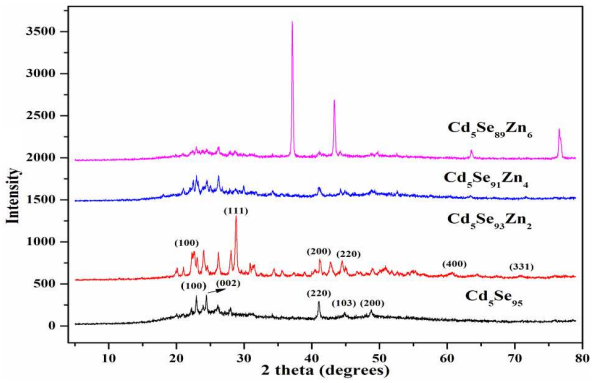

Fig. 1. XRD pattern of $Cd_5Se_{95-x}Zn_x$ (x = 0, 2, 4, 6) chalcogenide semiconductor.

valuable information about nature and structure of the samples. The copper target was used as a source of X-rays with $\lambda = 1.54$ Å (Cu K_{α_1}). Scanning angle was in the range of 5°–80°. A scan speed of 2°/min and a chart speed of 1 cm/min were maintained. The crystallite size of all the samples has been calculated from Scherrer's formula

$$D = k\lambda/\beta\cos\theta, \tag{1}$$

where D, λ, β and θ are the crystallite size, X-ray wavelength (=1.54 Å), full width at half maximum (FWHM) and Bragg's angle of reflection, respectively. The calculated grain sizes were found to increase with increase of Zn concentration. The value of strain (ε) and the dislocation density (δ) has been estimated using the following relation:

$$\varepsilon = \beta\cos\theta/4, \tag{2}$$

$$\delta = 1/D^2. \tag{3}$$

The intensity and sharp peak in XRD reveal good crystallinity which also confirms the stoichiometric nature of CdSeZn samples. The analysis of the spectrum shows the hexagonal wurtzite (W) structure in the whole range of composition studied which were well matched with the standard peaks (JCPDS No. 893682). Table shows the observed grain size D (nm), strain (ε), and dislocation density (δ) of the samples.

TABLE

Structural, ac conductivity parameter of $Cd_5Se_{95-x}Zn_x$ chalcogenide semiconductor at a temperature of 290 K and frequency 10 kHz.

Sample	2θ	Grain size D [nm]	Strain (ε) 10^{-3} lin m^4	Dislocation density δ [$\times 10^{16}$ m^{-2}]	σ_{ac}	m	W_m [eV]	ΔE [eV]
Cd_5Se_{95}	22.92	11.55	15.4	7.49	3.7×10^{-9}	–0.08	3.65	0.44
$Cd_5Se_{93}Zn_2$	28.82	20.71	86.1	2.33	1.6×10^{-8}	–0.36	0.87	0.63
$Cd_5Se_{91}Zn_4$	26.22	21.47	81.2	2.16	9.3×10^{-8}	–0.38	0.82	0.22
$Cd_5Se_{89}Zn_6$	37.11	17.66	101.1	3.21	4.6×10^{-8}	–0.44	0.71	0.59

3.2. Scanning electron microscopy (SEM) analysis

Surface morphology of the sample was investigated by SEM apparatus JEOL (Model JSM 6380). Figure 2 shows in the SEM image of the samples that it is clear that surface morphology changes due to incorporation of Zn in CdSe alloy. It is observed that the images of the sample are uniform and without any pinhole or cracks and the formation of conchoidal contours. The surface topology shows the cluster compound of nanoparticle of different size.

3.3. Fourier transform infrared (FTIR) studies

Using a Perkin-Elmer System (Spectrum RXI-Mid IR) an extensive FTIR is used to identify and characterize the organic species and to analyze the chemical bonding. The characteristics peaks exhibited by FTIR spectra in the frequency range 400–4400 cm^{-1} (mid-infrared range) of CdSeZn powder samples is shown in Fig. 3. The transmission peaks at 534 cm^{-1} and 1088 cm^{-1} are the Cd–Se bending vibrations and strong asymmetric vibrations of CdSe. The absorption around 1000 cm^{-1} is assigned to vibrational mode associated with mixed vibrations due to heteropolar bonds like Cd–Se, Se–Zn, and/or CdSeZn. From this study, it also observed that almost all existing peaks in FTIR spectra show slightly shifting behavior toward larger wave number as the crystal size increases.

4. Frequency dependence of ac conductivity

The ac conductivity $\sigma_{ac}(\omega)$ of $Cd_5Se_{95-x}Zn_x$ chalcogenide semiconductors is expressed as [18]:

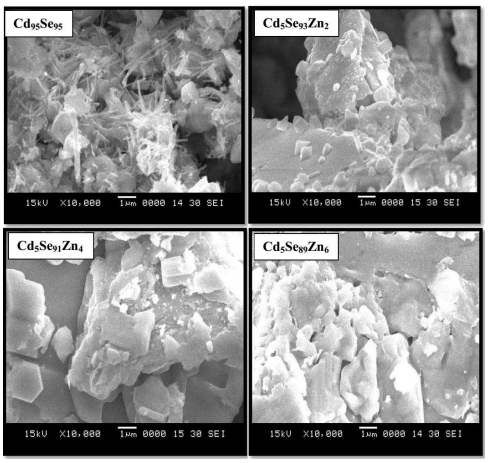

Fig. 2. SEM images for all the samples of $Cd_5Se_{95-x}Zn_x$ (x = 0, 2, 4, 6) chalcogenide semiconductor.

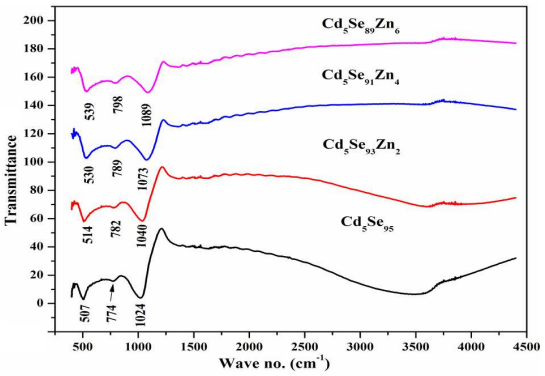

Fig. 3. FTIR spectra of $Cd_5Se_{95-x}Zn_x$ ($x = 0, 2, 4, 6$) chalcogenide semiconductor.

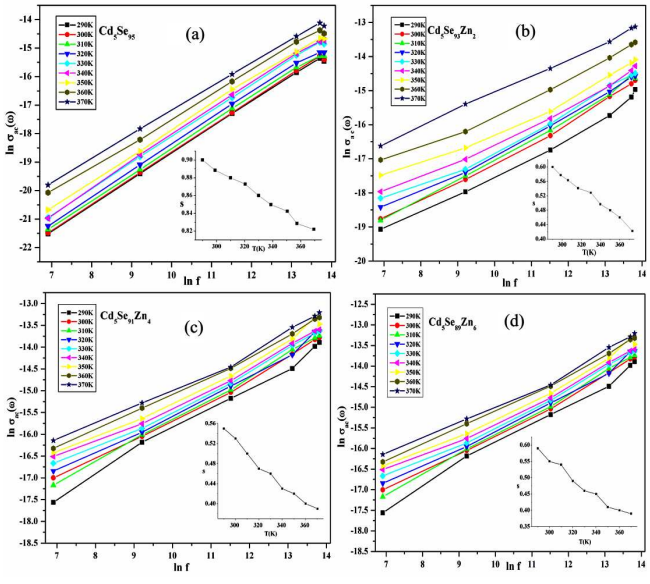

Fig. 4. (a)–(d) Frequency dependence of $\ln \sigma_{ac}(\omega)$ at different temperature and the inset figure shows the temperatures dependence of the parameters of s for $Cd_5Se_{95-x}Zn_x$ alloy.

$$\sigma_{ac}(\omega) = \sigma_t(\omega) - \sigma_{dc}(\omega) = A\omega^s, \quad (4)$$

Where ω is the angular frequency, $\sigma_t(\omega)$ is the measured total electrical conductivity, $\sigma_{dc}(\omega)$ is the dc electrical conductivity, s is the frequency exponent and A is constant dependent on temperature [19]. From Eq. (4), $\sigma_{ac}(\omega)$ increases linearly with frequency according to the relation caused by motion of charge carriers, tunneling or hopping between two equilibrium sites.

Figure 4a–d shows the relation between $\ln \sigma_{ac}(\omega)$ versus $\ln \omega$ for all samples at different temperatures (290–370 K), this figure reveals that $\sigma_{ac}(\omega)$ increases with increase of frequency through the measured temperature range and frequency range. Value of the frequency exponent s is obtained from the slopes of these curves. The temperature dependent parameter s for the investigated samples is shown in inset figure; it is clear that s decreases with increase of temperature. These results are in agreement with the correlated barrier hopping (CBH) [19–21] model, such behaviors were also reported by various researchers [22, 23]. According to this model, as suggested by Guintini et al. [24] the conduction occurs via bipolaron hopping process where two electrons simultaneously hop over the potential barrier between two defect charge states (D^+ and D) to form a dipole with relaxation energy, and the barrier height is correlated with interstice separation via a Coulombic interaction.

The expression for s obeys the formula

$$s = 1 - \frac{6kT}{W_m}, \quad (5)$$

where k Boltzmann is constant, T is temperature, W_m is the maximum barrier height at infinite interstice separation [25, 26]. This is called as the binding energy of the carrier in its localized sites [27]. The temperature dependent $\sigma_{ac}(\omega)$ at different frequencies for the present sample are shown in Fig. 5. It is clear from the figure that $\ln \sigma_{ac}(\omega)$ increases with reciprocal of temperature,

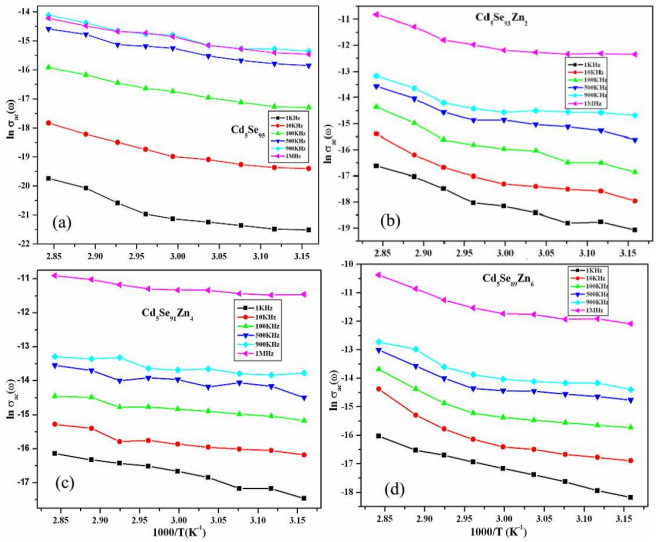

Fig. 5. (a)–(d) Temperature dependence of $\ln \sigma_{ac}(\omega)$ at different frequencies for $Cd_5Se_{95-x}Zn_x$ alloy.

this suggests that the $\sigma_{ac}(\omega)$ is thermally activated process with single activation energy from different localized state in the band gap. The activation energy [29] is calculated at different frequencies from the slope of these lines of Fig. 5 using the Arrhenius equation $\sigma_{ac}(\omega) = \sigma_0 \left(\frac{\Delta E}{kT}\right)$.

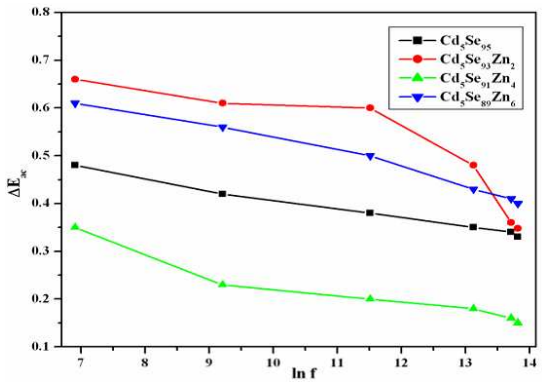

Fig. 6. Frequency dependence of ac activation energy (ΔE) for $Cd_5Se_{95-x}Zn_x$ alloy.

The frequency dependence of activation energy is shown in Fig. 6. It is clear from the figure that activation energy (ΔE) decreases with frequency, which may be due to increase of field frequency which enhances the electronic jump between localized states. Such observation has been reported by various authors in chalcogenide semiconductor [30–34]. The value of ΔE for the present sample at frequency of 10 kHz is shown in Table.

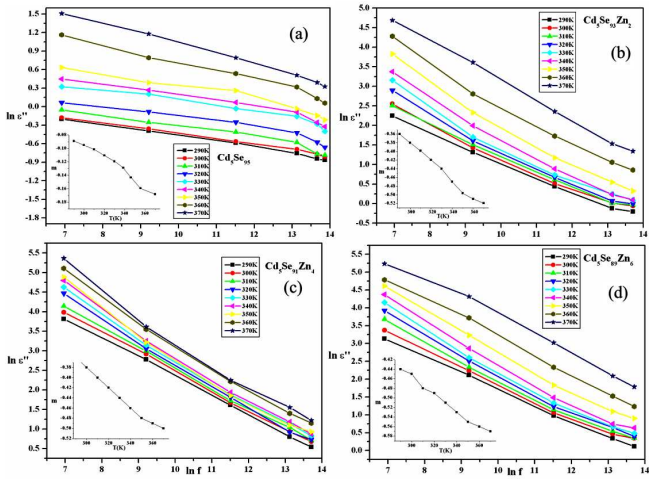

Fig. 7. Frequency dependence of $\ln \varepsilon''$ at different temperature and the inset figure shows the temperatures dependence of the parameters m for $Cd_5Se_{95-x}Zn_x$ alloy.

The data of the frequency dependence of ε'' can be represented as $\ln \varepsilon''$ vs. $\ln \omega$ as shown in Fig. 7a–d. This seems to fit the empirical relation [35, 36] $\varepsilon'' = B\omega^m$, where B is a constant and m is the frequency power factor.

Figure 7 enables us to calculate the value of power m from the negative slope of these lines. The variation of m with temperature is shown in the inset figures; it is clear from the figure that value of m decreases linearly with temperature, the experimental value of power

$$m = -4\pi kT/W_m. \tag{6}$$

W_m can be considered as work done in polarizing the dielectric, values of W_m can be calculated from Eq. (6) for all composition at fixed temperature 290 K is given in Table. These values are in good agreement with the theory of hopping of charge carriers over the potential barrier as suggested by Elliot.

5. Conclusion

XRD pattern of prepared $Cd_5Se_{95-x}Zn_x$ alloys are polycrystalline in nature. The temperature and frequency dependence of ac conductivity $\sigma_{ac}(\omega)$ are studied in the frequency range of 1 kHz–1 MHz and temperature range 290–370 K. Ac conductivity is found to obey the power law ω^s, where $s < 1$. $\sigma_{ac}(\omega)$ increases with increase of frequency through the measured temperature range, s decreases with increase of temperature. These results are in agreement with the correlated barrier hopping (CBH) model. According to this model the conduction occurs via bipolaron hopping process. Values of W_m were evaluated from the data of dielectric loss, which are in good agreement with the theory of hopping of charge carrier over a potential barrier between charged localized states.

Acknowledgments

I am highly thankful to the University Grants Commission (UGC), New Delhi (India) for providing me financial support in the form of Basic Scientific Research fellowship (BSR).

References

[1] A. Onozuka, O. Oda, *J. Non-Cryst Solids* **103**, 289 (1988).

[2] S. Kumar, M. Husain, M. Zulfequar, *Physica B* **387**, 400 (2007).

[3] H. Fritzsche, *J. Phys. Chem. Solids* **68**, 878 (2007).

[4] P. Pattanayak, S. Asokan, *Europhys. Lett.* **75**, 778 (2006).

[5] H.F. Hamann, M.O. Boyle, Y.C. Martin, M. Rooks, H.K. Wickramasinghe, *Nat. Mater.* **5**, 383 (2006).

[6] V. Balitska, O. Shpotyuk, H. Altenburg, *J. Non-Cryst. Solids* **352**, 4809 (2006).

[7] A. Ganjoo, H. Jain, C. Yu, R. Song, J.V. Ryan, J. Irudayaraj, Y.J. Ding, C.G. Pantano, *J. Non-Cryst. Solids* **352**, 584 (2006).

[8] S.A. Khan, M. Zulfequar, M. Hussain, *Solid State Commun.* **123**, 463 (2002).

[9] M.A. Majeed Khan, M. Zulfequar, M. Hussain, *J. Opt. Mater.* **22**, 21 (2003).

[10] P. Sharma, S.C. Katyal, *Physica B* **403**, 3667 (2008).

[11] E. Marquez, T. Wagner, J.M. Gonzalez-Leal, A.M. Bernal-Olive, R. Prieto-Aleton, R. Jimenez-Garay, P.J.S. Ewen, *J. Non-Cryst. Solids* **274**, 62 (2000).

[12] E. Sagbo, D. Houphouet-Boigny, R. Eholic, J.C. Jumas, J. Olivier-Fourcadu, M. Mouriu, J. Rivet, *J. Solid State Chem.* **113**, 145 (1994).

[13] A.A. Simashkevich, S.D. Shutov, *Semiconductor (USA)* **28**, 80 (1994).

[14] A. Vidourek, L. Tichy, M. Vlcek, *Mater. Lett. (Netherlands)* **22**, 59 (1995).

[15] F. Salam, J.C. Giuntini, S.S. Soulayman, J.V. Zanchetta, *Appl. Phys. A Mater. Sci. Process (Germany)* **60**, 309 (1995).

[16] A. Daoudi, J.C. Levet, M. Potel, H. Noel, *Mater. Res. Bull. (USA)* **31**, 1213 (1996).

[17] A.N.R. Long, *Adv. Phys.* **31**, 553 (1981).

[18] S.R. Elliott, *Adv. Phys.* **36**, 135 (1987).

[19] A.K Jonscher, *Nature* **267**, 673 (1977).

[20] S.R. Elliott, *Philos. Mag. B* **36**, 1291 (1977).

[21] A.R. Long, *Adv. Phys.* **31**, 553 (1982).

[22] A.M. Farid, H.E. Atyia, N.A. Hegab, *Vacuum* **80**, 284 (2005).

[23] R.S. Kundu, K.L. Bhatia, N. Kishore, *Philos. Mag. B* **72**, 513 (1995).

[24] J.C. Guintini, J.V. Zanchetta, D. Jullien, R. Enolie, P. Houenou, *J. Non-Cryst. Solids* **45**, 57 (1981).

[25] G.E. Pike, *Phys. Rev. B* **6**, 1572 (1972).

[26] V.K. Bhatnagar, K.L. Bhatia, *J. Non-Cryst. Solids* **119**, 214 (1990).

[27] B.K. Chaudhuri, J.K. Chaudhuria, K.K. Som, *J. Phys. Chem. Solids* **50**, 1149 (1989).

[28] L.G. Austin, N.F. Mott, *Adv. Phys.* **18**, 41 (1969).

[29] C. Angell, *Annu. Rev. Phys. Chem.* **43**, 693 (1992).

[30] F.A. Abdel Wahab, M. Abdel-Baki, *J. Non-Cryst. Solids* **355**, 2239 (2009).

[31] H.E. Atyia, *Vacuum* **81**, 590 (2007).

[32] M.M. Abdel-Aziz, M.A. Afifi, H.H. Labib, E.G. El-Metwally, *Acta Phys. Pol. A* **98**, 393 (2000).

[33] N.A. Hegab, M.A. Afifi, H.E. Atyia, M.I. Ismael, *Acta Phys. Pol. A* **119**, 416 (2011).

[34] N.A. Hegab, A.E. Bekheet, M.A. Afifi, L.A. Wahaba, H.A. Shehata, *J. Ovonic Res.* **3**, 71 (2007).

[35] N.A. Hegab, H.M. El-Mallah, *Acta Phys. Pol. A* **116**, 1048 (2009).

[36] J.C. Guintini, J.V. Zandieha, *J. Non-Cryst Solids* **34**, 57 (1979).